

Highly Scalable Neuromorphic Hardware with 1-bit Stochastic nano-Synapses

Omid Kavehei

Centre for Neural Engineering

Department of Electrical and Electronic Engineering

The University of Melbourne, Victoria 3010, Australia

Email: omid.kavehei@unimelb.edu.au

Abstract

This work presents a highly scalable neuromorphic hardware based on crossbar array of 1-bit resistive cross points as distributed synapses with in-situ stochastic characteristic. The network shows a robust performance in emulating selectivity of synaptic potentials in neurons of primary visual cortex to the orientation of a visual image. The proposed model could be configured to accept a wide range of nanodevices. This work presents a highly scalable neuromorphic hardware based on crossbar array of 1-bit resistive cross points as distributed synapses with in-situ stochastic characteristic. The network shows a robust performance in emulating selectivity of synaptic potentials in neurons of primary visual cortex to the orientation of a visual image. The proposed model could be configured to accept a wide range of nanodevices.

I. INTRODUCTION

Cognitive computing with nanoelectronics is an emerging field of research that aims to fill the gap between CPU's performance and mammalian brains. CPUs outperform human brain in almost all tasks that involve deterministic computation. They, however, lack a very important feature, which is the ability to learn and work with unreliable building blocks. This unique characteristic of mammalian brains has attracted attention of scientists from different fields including electronic engineering. In the late 1980s, Caver Mead, and later Eric Vittoz, envisioned the use of very-large-scale integration (VLSI) systems and analog circuits to mimic neuro-biological architectures of nervous system [1], [2].

It is believed that the hippocampus of a mammalian brain is responsible for memory and learning. It consists of neurons and chemical synapses [3]. On the contrary to the common belief that neural systems, including hippocampus, are analog systems, there are several neurobiological evidence for existence of discrete changes of synaptic strength at least in some subfields in hippocampus [4]. There are also a number of

research that suggest efficient learning with digital synapses [5], [6]. Therefore, even though an analog approach promises more power efficiency, a digital implementation improves design simplicity, it does not have limited scalability of analog implementations, it is less costly, small, and by far more integrable, hence, practically the best way, if not the only way, to implement highly scalable neuromorphic systems [7]. For instance, analog designs allow low-voltage operation, which then requires larger sensing circuitry and also does not necessarily support reasonable throughputs (spikes/s). It is expected that massively parallel, reliable, scalable, and potentially ultra-energy efficient cognitive systems could be implemented using 1-bit stochastic digital synapses.

A deterministic approach, has its focus on ‘more number of bits per synapse’ to allow a more precise implementation of a learning rule, and generally suffers multiple data conversion (ADCs and DACs). On the other side, emerging artificial synapses, such as RRAM (resistive RAM), CBRAM (conductive bridge RAM), PCM (phase change memory) and atomic switches, in their analog operating mode, have issues like (i) complicated programming pulse-schemes to achieve more intermediate states, which sometimes only exists in one switching direction (either OFF-ON or ON-OFF), and (ii) the problem of resistance drift or state retention [8], [9]. Technologies like STT-MRAM (spin-transfer torque magnetoresistive RAM) and MeRAM (magnetoelectric RAM) also show existence of multi-stable states, but the resistance margins are extremely narrow [10], which make them impractical for conventional analog neuromorphic computing. A workaround to these problems is to make the synaptic transmission a probabilistic process [8], [11]–[14]. This stochastic behavior can be achieved either in-situ or ex-situ.

This work uses the in-situ stochastic switching characteristic of RRAM devices to present a technology independent approach to implement a highly scalable neuromorphic hardware that is capable of emulating sensitivity of synaptic potentials in neurons of primary visual cortex to the orientation of a visual image. Considering the fact that all underlying physical mechanisms of state switching in RRAM, CBRAM and PCM are based on changing material properties (moving ions or crystallization-amorphous phase transition), it can be envisioned that even in near future, their yield and variation (including both spatial and cycle-to-cycle, C2C, variations), remains substantially larger than their CMOS counterparts. Therefore, a probabilistic approach is one of the most practical and highly scalable designs for neuromorphic hardware and logic operations with nanoelectronics.

II. STOCHASTIC NANO-SYNAPSE

A. Stochastic finite state machines

Stochastic binary switching is common between the emerging memory technologies. This behavior normally occurs under certain condition, which is called “weak” programming. Although, the weak programming condition is different across technologies, a technology independent approach is presented to pave the way for further unification of system-level behavior based on above mentioned technologies.

Stochastic switching of a nanodevice could be treated as a black-box; a generalized model, which is identified by a set of inputs and outputs. Fig. 1 provides an overview of the model. Outputs $x_{(n+1)}$ and $G_{(n+1)}$ represent next state and next conductance of the device, which both are probabilistic and their values are defined by the functions $f(\cdot)$ and $g(\cdot)$, respectively. Once $x_{(n+1)}$ is determined, $G_{(n+1)}$ is calculated using an experimentally verified distribution (in this paper, log-normal) of ON and OFF state resistances. The function $f(\cdot)$ is a function of voltage/current, time (here pulse-width) and operating temperature. Small updates in $g(\cdot)$ is independent of function $f(\cdot)$ output, which means if $x_n = x_{(n+1)}$, G_n and $G_{(n+1)}$ may not be equal.

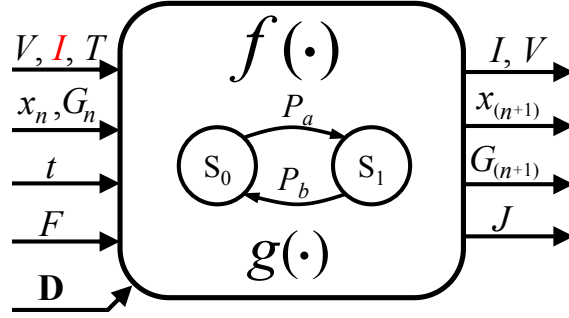


Fig. 1: A generalized form of modeling in-situ stochastic behavior of a given device (in this paper, RRAM). Inputs consist of applied voltage, V (or current, I), operating temperature, T , signal pulse-width, t , initial state x_n and initial conductance G_n . Device type and relevant fitting parameters are given by D . The model accepts cross-point yield as a defect rate input F (not to be confused with the material's point defect). Function $f(\cdot)$ defines switching probability and function $g(\cdot)$ defines conductance value randomness under a given C2C variation distribution. Switching probabilities are defined as P_a and P_b for switching from logic state '0', S_0 , to logic state '1', S_1 , and from logic state '1' to logic state '0', respectively. Outputs are current and voltage responses, next state ($x_{(n+1)}$), next conductance ($G_{(n+1)}$), as well as total consumed energy J of the whole operation to performing a programming or sensing, regardless of its success.

B. Probabilistic plasticity

Experimental data on voltage, pulse-width and temperature dependency of a resistive memory systems is gathered from [8], [12]–[18]. Device switching probability is defined as a strong function of applied voltage, ΔV , and time, Δt . For simplicity, temperature dependency and switching threshold variation of the device are considered to have an overall impact on the switching probability, therefore, their impact are not discussed as independent variables. Fig. 2 demonstrates switching probability of the SET ($S_0 \rightarrow S_1$) and RESET ($S_1 \rightarrow S_0$). Under similar condition, a SET is more likely than a RESET. Given that the $S_0 \rightarrow S_1$ seems more likely, it is possible to modulate the probabilistic LTP using a complicated learning rule, ΔW , where W represents synaptic weight that is bounded between a maximum and a minimum limits, through a different programming pulse-scheme for LTP, which makes the design more complex. Experimentally verified information regarding

the switching probability model are given in [13]. The switching probability is achieved by integrating a Poisson-like distribution, which is in an excellent agreement with the hypothesis of thermodynamic activation during filament formation over a dominant energy barrier in RRAM devices.

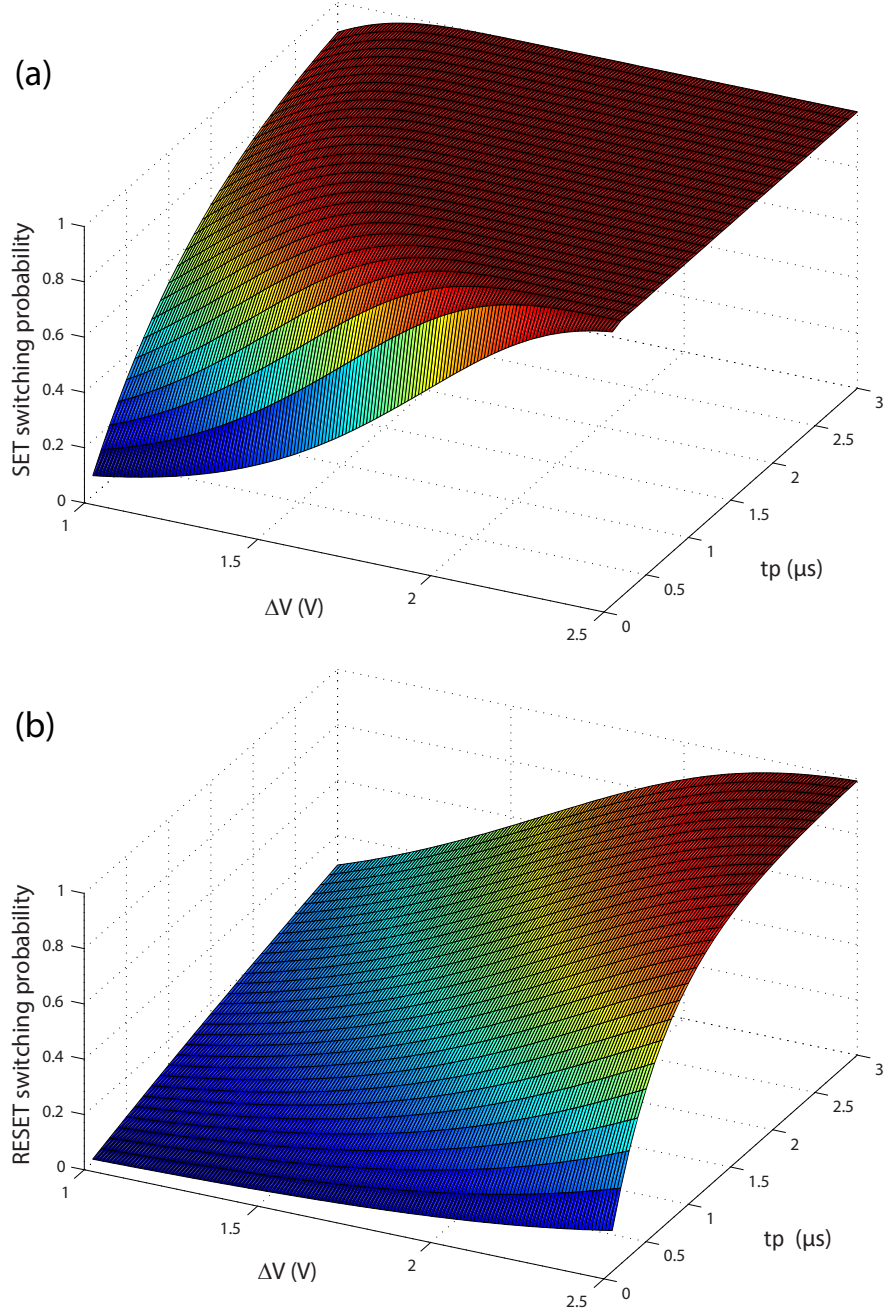


Fig. 2: Output of function $f(\cdot)$. (a) demonstrates SET switching probability and (b) shows RESET switching probability. t_p represents applied voltage pulse-width.

This stochastic behavior in combination with ΔW results a probabilistic LTP (long-term potentiation)

and LTD (long-term depression), which is a function of time difference (Δt) between a pre- and a post-synaptic spike (probabilistic spike timing-dependent plasticity, pSTDP) or their difference in voltage (ΔV). Stochastic change of the device state can also occur under a sequence of applied pulses with a fixed t_p . The probabilistic plasticity, which defines the probability of change in the device state, is shown in Fig. 3. Here ΔW is defined as

$$\Delta W = \begin{cases} 1, & \text{if } \Delta t > 0, \\ -1, & \text{if } \Delta t < 0. \end{cases} \quad (1)$$

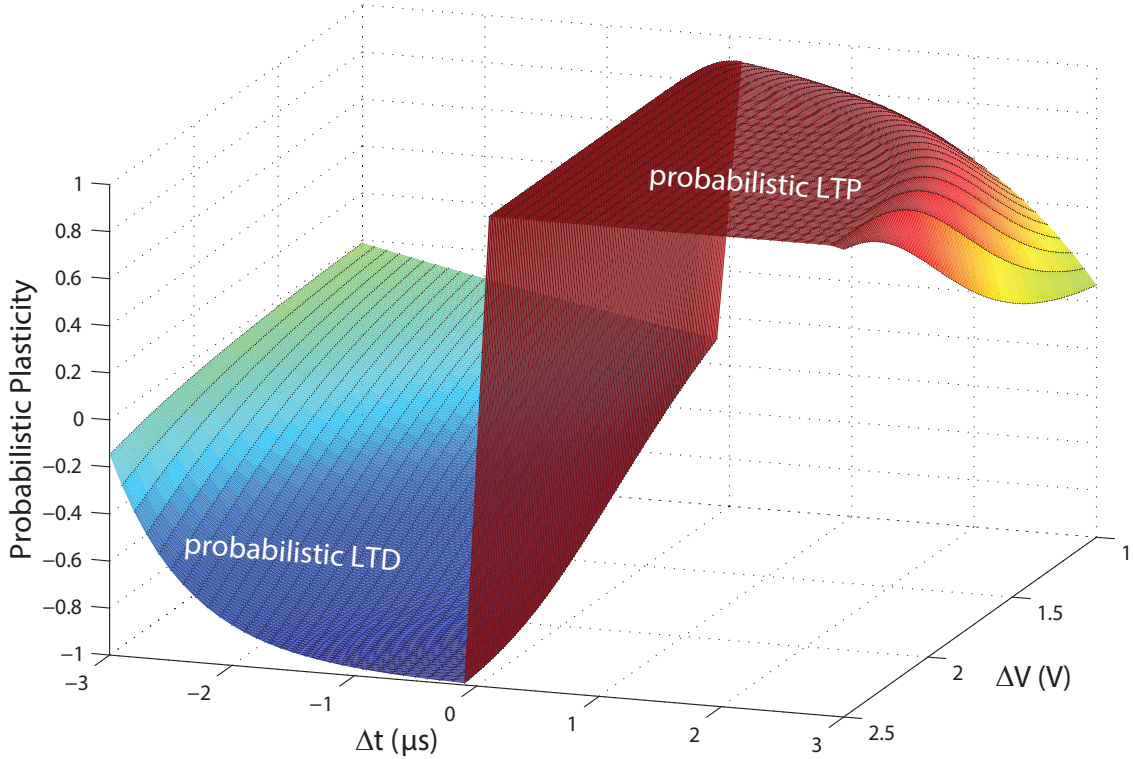


Fig. 3: Probabilistic plasticity that is ‘solely’ implemented using the in-situ stochastic switching of a 1-bit synapse.

It can be shown that a simple form of ΔW , like Eq. (1), is enough to successfully implement a robust and reliable selectivity task. There is a significant cycle-to-cycle resistance variation. This uncertainty is defined and verified using the function $g(\cdot)$. The RRAM and CBRAM devices have experimentally shown log-normal distribution of ON and OFF state resistances. Fig. 4 illustrates high and low resistance variation of a RRAM device for more than 4000 switching cycles. In some devices, like [12], OFF state resistances may show wider variation due to the uncontrolled metallic filament dissolution.

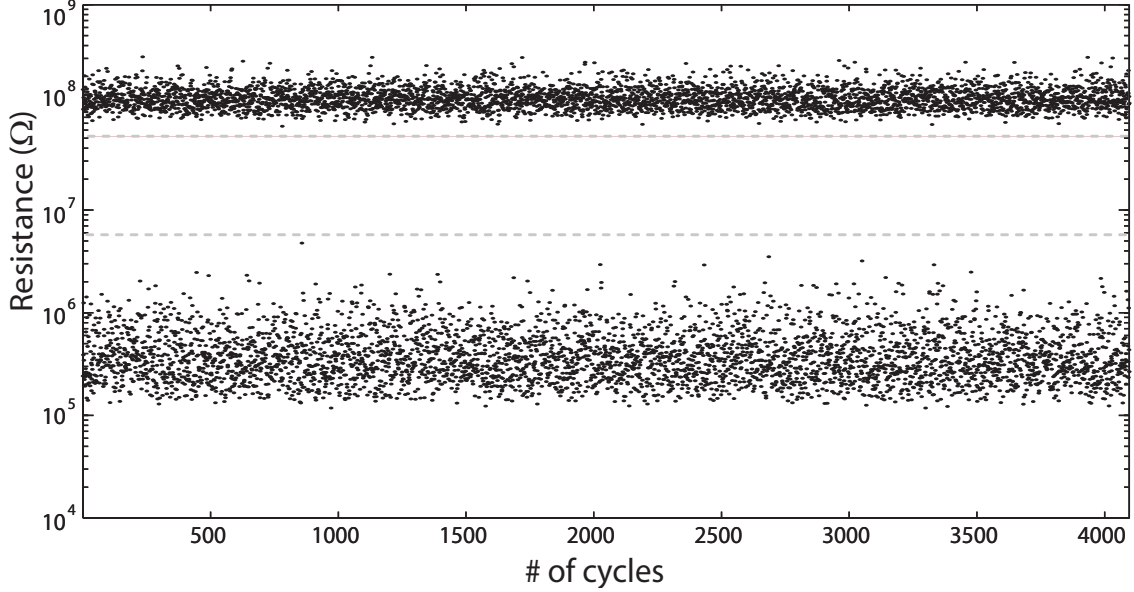


Fig. 4: OFF and ON resistance variation of a single RRAM for > 4000 switching cycles. This behavior is captured by $g(\cdot)$.

III. ORIENTATION SENSITIVITY

A two layer neural network is implemented with 64×64 -pixel binary visual images. Inputs were generated using a Gabor-like function to produce more than a thousand, randomly centered, receptive fields. Each input pixel drives an input neuron that spikes if the pixel represents ‘1’. There are nine output neurons that are fully connected to all input neurons through one-bit resolution stochastic RRAM connections. Therefore, 36,864 synapses are available that are randomly programmed and some are faulty. Faulty device patterns, random initial state, and some of the visual inputs are shown in Fig. 5. Output neurons are integration-and-fire neurons that are connected to each other through inhibitory connections, which form a winner-takes-all network. Output neurons could be configured to implement Hebbian, anti-Hebbian, STDP, and anti-STDP learning with a support for a programmable refractory period. The system implements an unsupervised competitive learning that is capable of accepting a wide range of input patterns, including visual and auditory with or without preprocessing.

Energy per spike is an important factor. The model is able to estimate both dynamic switching energy and static leakage power through unselected devices and sneak current paths with or without selector devices. Although, there is little experimental information available regarding spatial variation (device-to-device), the model aims to consider overall impact of such variation with some worst-case assumptions.

During training, inputs were shown to the network and each was repeated several times. After training, as shown in Fig. 6a, output neurons become sensitive to several orientations. Fig. 6b shows that the system was

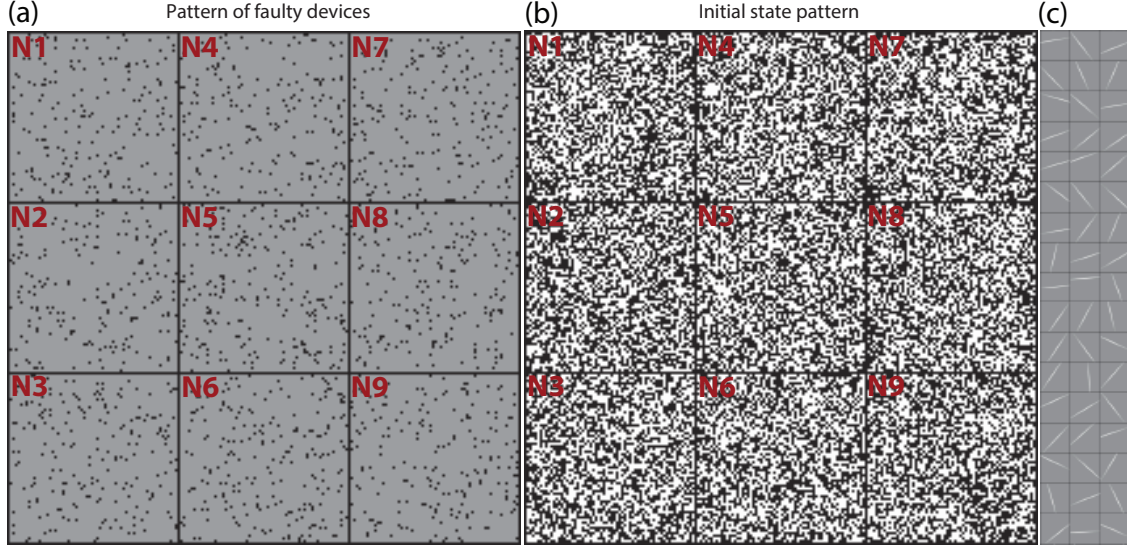


Fig. 5: (a) shows device defect patterns. A black dot represents a faulty device, which is not able to switch (either stuck-at-ON or -at-OFF). Yield is 95% and 70% of faulty devices are stuck-at-ON. (b) demonstrates initial random patterns of ON and OFF devices. Black pixels show OFF state devices and white pixels are ON device. Half of the functioning devices are randomly programmed as ON, and the remaining as OFF. (c) some of the randomly generated input patterns are shown here.

not sensitive to any angle prior to learning. The system sensitivity to particular angles of the visual input patterns is demonstrated in Fig. 6c. One of the main parameters of designing the system is the dynamic tuning of the output neurons' firing threshold, which is not the focus of this paper. The training process were repeated with different threshold tuning approaches and a range of initial conditions, device variation, and defect patterns. The system continues to perform reliably under extreme yield (defect rate is $> 20\%$) and variability assumptions, where the function $f(\cdot)$ output varies within 0.1 probability (3σ) around its nominal value. Implementing such system with low-power synapses would produce an ultra-high energy efficient and highly scalable system with an energy consumption of < 1 pJ/spike.

IV. CONCLUSION

The implemented neuromorphic system is (i) highly scalable, (ii) easily mappable on the current crossbar memory architecture, (iii) not sensitive to device variation, (iv) working reliably with or without selector devices, (v) potentially very high energy efficient, and (vi) potentials for high throughput applications. Each training process, in this case, demands for an endurance requirement in the order of $> 20k$ cycles, which is well within the current reported endurance of RRAM, CBRAM, PCM, STT-MRAM, MeRAM, and atomic switches. Currently, there is no conventional nonvolatile memory (including Flash) that satisfy this dynamic endurance requirement, therefore, ex-situ stochastic approaches in CMOS (e.g. random number

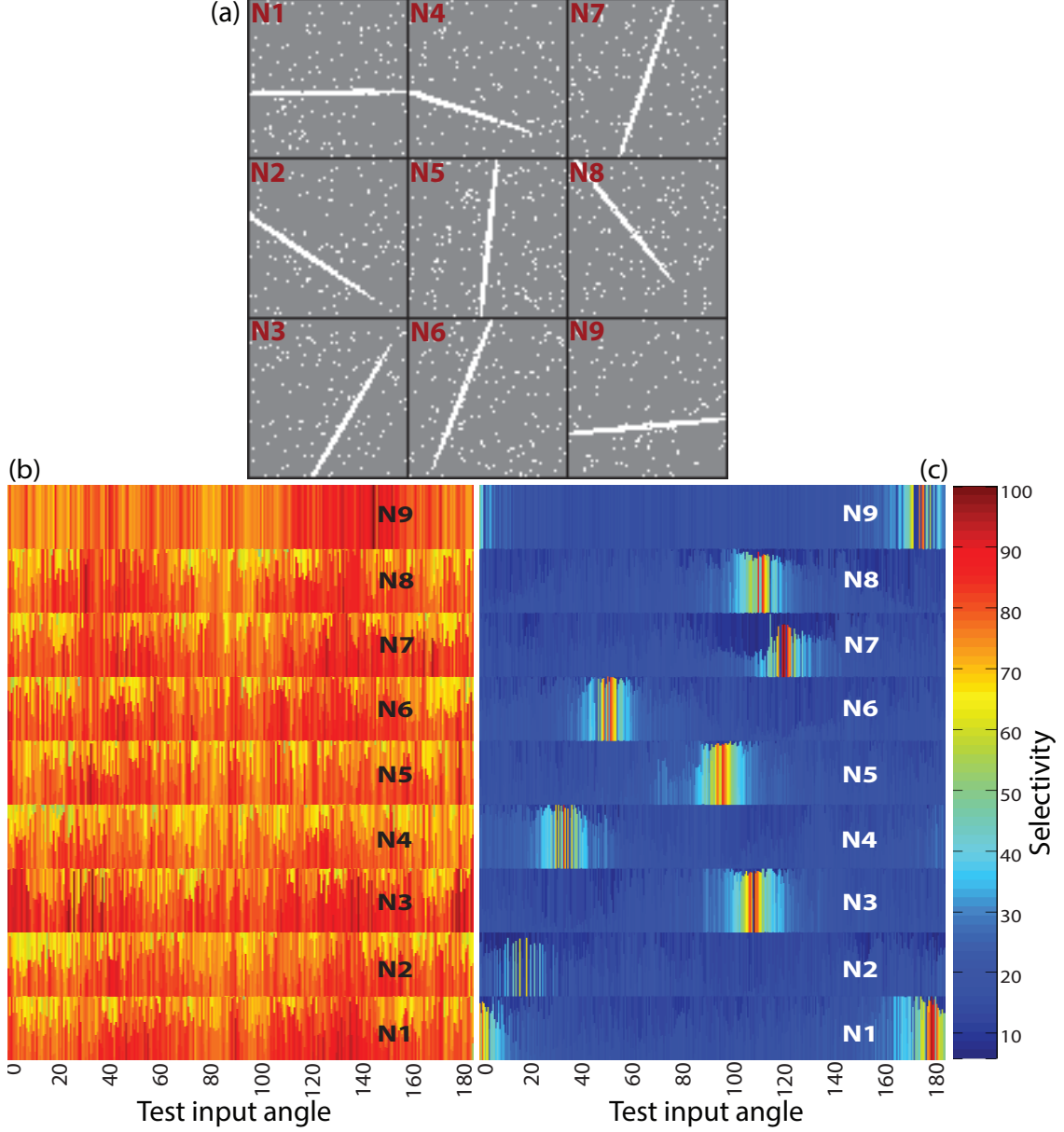


Fig. 6: (a) output neurons after training. Random white pixels are either faulty stuck-at-ON devices or ON state devices. Output neurons' sensitivity to $> 10,000$ test patterns before training (in response to Fig. 5b) and after training are shown in (b) and (c), respectively.

generator), dynamically updates digital synaptic weights in volatile SRAM. Cost-wise, implementing such network with RRAM, CBRAM, PCM, and atomic switches may be cheaper relative to STT-MRAM and MeRAM. However, rapid progress of these technologies promises high energy efficient memory systems, which makes the cost-energy trade-off of these devices more attractive in the near future. Modeling accuracy can be further improved through systematic studies like [13].

ACKNOWLEDGEMENTS

The author would like to thank Dr Shimeng Yu for his insightful discussions on memory technologies and Ms Nina Erfanian Saeedi for her comments on the neural network implementation and selectivity.

REFERENCES

- [1] C. Mead *et al.*, *Analog VLSI implementation of neural systems*. Springer, 1989.
- [2] E.-A. Vittoz, “Analog VLSI implementation of neural networks,” in *IEEE International Symposium on Circuits and Systems*, 1990, pp. 2524–2527.
- [3] H. Lim *et al.*, “Short-term memory of TiO₂-based electrochemical capacitors: empirical analysis with adoption of a sliding threshold,” *Nanotechnology*, vol. 24, no. 38, p. 384005, 2013.
- [4] D.-H. O’Connor *et al.*, “Graded bidirectional synaptic plasticity is composed of switch-like unitary events,” *Proceedings of the National Academy of Sciences*, vol. 102, no. 27, pp. 9679–9684, 2005.
- [5] S. Fusi, “Hebbian spike-driven synaptic plasticity for learning patterns of mean firing rates,” *Biological Cybernetics*, vol. 87, no. 5–6, pp. 459–470, 2002.
- [6] W. Senn *et al.*, “Convergence of stochastic learning in perceptrons with binary synapses,” *Physical Review E*, vol. 71, no. 6, p. 061907, 2005.
- [7] J.-S. Seo *et al.*, “A 45nm CMOS neuromorphic chip with a scalable architecture for learning in networks of spiking neurons,” in *IEEE Custom Integrated Circuits Conference*, 2011, pp. 1–4.
- [8] D. Kuzum *et al.*, “Synaptic electronics: materials, devices and applications,” *Nanotechnology*, vol. 24, no. 38, pp. 382 001–382 001, 2013.
- [9] M. Suri *et al.*, “Impact of PCM resistance-drift in neuromorphic systems and drift-mitigation strategy,” in *IEEE/ACM International Symposium on Nanoscale Architectures*, 2013.
- [10] K. Wang *et al.*, “Low-power non-volatile spintronic memory: STT-RAM and beyond,” *Journal of Physics D: Applied Physics*, vol. 46, no. 7, p. 074003, 2013.
- [11] B. Walmsley *et al.*, “The probabilistic nature of synaptic transmission at a mammalian excitatory central synapse,” *Journal of Neuroscience*, vol. 7, no. 4, pp. 1037–1046, 1987.
- [12] M. Suri *et al.*, “CBRAM devices as binary synapses for low-power stochastic neuromorphic systems: Auditory (Cochlea) and visual (Retina) cognitive processing applications,” in *IEEE International Electron Devices Meeting*, 2012, pp. 3–10.
- [13] S. Gaba *et al.*, “Stochastic memristive devices for computing and neuromorphic applications,” *Nanoscale*, vol. 5, pp. 5872–5878, 2013.
- [14] S. Yu *et al.*, “A low energy oxide-based electronic synaptic device for neuromorphic visual systems with tolerance to device variation,” *Advanced Materials*, vol. 25, no. 12, pp. 1774–1779, 2013.
- [15] O. Kavehei *et al.*, “Fabrication and modeling of Ag/TiO₂/ITO memristor,” in *IEEE International Midwest Symposium on Circuits and Systems*, 2011, pp. 1–4.
- [16] —, “An associative capacitive network based on nanoscale complementary resistive switches for memory-intensive computing,” *Nanoscale*, vol. 5, no. 11, pp. 5119–5128, 2013.
- [17] J.-K. Park *et al.*, “Analysis of resistance variations and variance-aware read circuit for cross-point ReRAM,” in *IEEE International Memory Workshop*, 2013, pp. 112–115.
- [18] M.-F. Chang *et al.*, “A high-speed 7.2-ns read-write random access 4-Mb embedded resistive RAM (ReRAM) macro using process-variation-tolerant current-mode read schemes,” *IEEE Journal of Solid-State Circuits*.